Influence of Microwave Power on the Characteristics of Carbon Dots Synthesized from Corn Husks



N. Zulkifli[1], H. Alwi[1,2*], S. M. Sauid[1], M. F. Sarulan[1], N. Wahid[1]

[1]School of Chemical Engineering, College of Engineering, Universiti Teknologi MARA Shah Alam, 40450 Shah Alam, Selangor, Malaysia.
[2]Food Process Engineering Research Group (FOPERG) Universiti Teknologi MARA Shah Alam, 40450 Shah Alam, Selangor, Malaysia.



ABSTRACT: Carbon nanomaterials, particularly carbon dots (CDs), are recognized for their remarkable properties such as fluorescence, biocompatibility, and ease of surface functionalization, making them suitable for bioimaging, drug delivery, and environmental monitoring. Despite their potential, there remains a significant gap in understanding how synthesis methods, particularly the microwave-assisted method, influence their properties. The microwave-assisted method offers rapid, energy-efficient, and scalable synthesis by subjecting precursor materials to microwave radiation, resulting in the swift formation of CDs. This study focuses on synthesizing corn husk-carbon dots (CH-CDs) using varying microwave power levels of 450 W, 600 W, 750 W, and 900 W. Characterization techniques include Ultraviolet-visible (UV-Vis) spectroscopy to analyze absorption properties, zeta potential analysis to measure particle stability in the dispersed system, and Fourier transform infrared (FTIR) spectroscopy to identify functional groups. Results indicated that higher microwave power enhances stability, with CH-CDs synthesized at 900 W exhibiting the most negative zeta potential values, signifying increased electrostatic repulsion and stability. UV-VIS spectra exhibited a distinct absorption peak at 292 nm and a weaker peak between 300-360 nm, while FTIR analysis revealed the presence of key functional groups like hydroxyl and carbonyl, essential for surface functionality, suggesting that microwave-assisted synthesis at optimal power levels can significantly influence carbon dots properties.

KEYWORDS: Carbon Dots, Corn Husk, Microwave-assisted Method, Power Levels, Characterization

[Received Oct. 22, 2024; Revised Dec. 3, 2024; Accepted Dec. 15, 2024] Print ISSN: 0189-9546 | Online ISSN: 2437-2110

I. INTRODUCTION

Carbon nanomaterials (CNMs) are classified based on their dimensional structures into zero-dimensional (0D), one-dimensional (1D), and two-dimensional (2D), with certain types extending into three-dimensional (3D) forms. The 0D category consists of carbon quantum dots (CQDs) and fullerenes, while 1D encompasses carbon nanotubes (CNTs) and carbon nanohorns, and the two-dimensional (2D) includes graphene and carbon nanoribbons (Zakaria et al., 2022). Additionally, 3D structures like carbon nanofibers (CNFs) and carbon nanofoams represent another important class of carbon nanomaterials, as detailed in Table 1 (Liu et al., 2018; Zakaria et al., 2022). Among the diverse range of carbon nanomaterials, particularly carbon dots (CDs), have garnered significant attention due to their unique properties and versatile applications, such as strong fluorescence, biocompatibility, and the ability to easily modify their surface. These properties make carbon dots highly suitable for numerous applications, including bioimaging, drug delivery, and environmental monitoring (Gedda et al., 2023).

The synthesis of carbon dots can be achieved through various methods, each offering distinct benefits and challenges. Hydrothermal synthesis allows for precise control of growth in high-temperature aqueous environments, while pyrolysis provides versatility in selecting precursors and tailoring surface chemistry (Sim et al., 2019; Yadav et al., 2023). Electrochemical synthesis is notable for its simplicity and scalability, and solvothermal synthesis offers control over the morphology and surface characteristics of the carbon dots (Sharma & Das, 2019). Laser ablation and ultrasonic methods provide fast and efficient routes to synthesis (Kurian & Paul, 2021). Among these methods, the microwave-assisted approach stands out for its speed, energy efficiency, and scalability. This method uses microwave radiation to form carbon dots from precursor materials, yielding advantages such as enhanced optical properties, improved yield, and uniform particle size (Kang et al., 2020). The power levels used during microwave irradiation play a crucial role in modifying the structural and optical properties of the carbon dots, emphasizing the importance of optimizing synthesis parameters to achieve the desired outcome

*Corresponding author: habsahalwi@uitm.edu.my

doi: http://dx.doi.org/10.63746/njtd.v22i3.3037

Table 1: The classifications and properties of carbon nanomaterials.

Classes of carbon nanomaterials	Types of carbon nanomaterials	Properties	Applications
0-D	Carbon quantum dots (CQDs)	❖ CQDs are small carbon nanoparticles with sizes less than 10 nm. ❖ They possess quantum confinement effects and exhibit unique optical and electronic properties (Soni & Pamidimukkala, 2018). ❖ Applications of CQDs include bioimaging, sensors, optoelectronics, and photocatalysis.	❖ **Bioimaging**: High fluorescence makes CQDs ideal for cell tracking and imaging (Cui et al., 2021). ❖ **Sensors**: Used in chemical and biological sensors due to their sensitivity and selectivity. ❖ **Optoelectronics**: Suitable for light-emitting diodes (LEDs) and solar cells. ❖ **Photocatalysis**: Effective water splitting and degradation of organic pollutants under light exposure (Cui et al., 2021).
	Fullerenes	❖ Fullerenes are closed-cage structures consisting of carbon atoms, resembling spheres, ellipsoids, or tubes (Zhu et al., 2019). ❖ The most common fullerene is Buckminsterfullerene (C60), which has a soccer ball-like structure. ❖ They have potential applications in areas such as medicine, materials science, and electronics.	❖ **Medicine**: Potential for drug delivery, antioxidants, and antiviral activity (Ayawei et al., 2018). ❖ **Materials Science**: Used in the synthesis of advanced composites and coatings. ❖ **Electronics**: Employed in organic photovoltaics, transistors, and superconductors (Bhakta et al., 2020).
1-D	Carbon nanotubes (CNTs)	❖ CNTs are cylindrical structures made of rolled-up graphene sheets (Porto et al., 2020). ❖ They can be single walled (SWCNTs) or multi-walled (MWCNTs), depending on the number of layers.	❖ **Electronics**: Used in transistors, conductive films, and displays due to high electrical conductivity (Peng et al., 2014). ❖ **Structural Reinforcement**: Improve the strength and durability of composites in aerospace and construction. ❖ **Energy Storage**: Key component in batteries, supercapacitors, and fuel cells.
2-D	Graphene	❖ Graphene is a single layer of carbon atoms arranged in a two-dimensional honeycomb lattice (Zhu et al., 2019). ❖ It exhibits remarkable electrical conductivity, mechanical strength, and flexibility. ❖ Graphene has diverse applications, including electronics, energy storage, sensors, and biomedical devices.	❖ **Electronics**: Found in transistors, flexible displays, and touchscreens. ❖ **Energy Storage**: Integral to high-performance batteries, supercapacitors, and hydrogen storage systems (Olabi et al., 2021). ❖ **Sensors**: Extremely sensitive for gas, chemical, and biological detection. ❖ **Biomedical Devices**: Used for drug delivery, biosensors, and tissue scaffolds due to their biocompatibility and mechanical properties (Han et al., 2019).
	Carbon nanoribbon	❖ Carbon nanoribbons are one-dimensional carbon	❖ **Electronics**: Serve as components in nanoscale transistors, memory devices, and semiconductors.

		nanomaterials that exhibit a ribbon-like morphology. ❖ They are essentially narrow strips of graphene, possessing widths on the nanometer scale and lengths that can vary from a few nanometers to micrometers. ❖ Carbon nanoribbons can be classified into two main types based on their edge structures: armchair-edge nanoribbons and zigzag-edge nanoribbons. The edge structure significantly influences their electronic properties (Poklonski et al., 2012).	❖ **Spintronics**: Useful in spin-based electronic devices due to unique edge magnetic properties (Cao et. Al, 2020). ❖ **Energy Storage**: Incorporated into batteries and supercapacitors for improved performance.
3-D	Carbon nanofibers (CNFs)	❖ CNFs are fibrous structures composed of carbon atoms arranged in a graphitic structure. ❖ They can be produced by various methods, including electrospinning and chemical vapor deposition (Yang et al., 2023). ❖ CNFs are utilized in aerospace, automotive, energy storage, and biomedical applications.	❖ **Energy Storage**: Used in anodes for batteries and electrodes for supercapacitors (Mohamed, 2019). ❖ **Biomedical Applications**: Act as scaffolds for tissue engineering and wound healing (Mohamed, 2019). ❖ **Environmental Applications**: Effective in pollutant filtration and oil-water separation.
	Carbon nanofoams	❖ Carbon nanofoams are three-dimensional porous structures composed of interconnected carbon nanoparticles or nanotubes (Frese et al., 2016). ❖ They have a sponge-like morphology characterized by a network of interconnected pores.	❖ **Catalysis**: Provide a high surface area for catalytic reactions in chemical and electrochemical processes (Louis, 2009). ❖ **Thermal Insulation**: Serve as excellent heat-resistant materials in aerospace and industrial applications (Forest, 2015). ❖ **Environmental Applications**: Used in gas storage, pollutant adsorption, and water purification systems.

This research area is gaining attention for its potential to utilize biobased resources for wastewater remediation, addressing critical concerns regarding the presence of toxic and carcinogenic compounds in wastewater (Saeed et al., 2019). The use of dyes and pigments in various industries significantly contributes to environmental pollution, with large amounts of these compounds entering the environment through industrial effluents. However, prior studies have explored the use of carbon dots produced from *Azadirachta Indica* leaves, which were found to remove up to 83% of the dye from wastewater (Thiruketheeswaranathan & Somasiri, 2021). Another study by Ray et al. (2019), demonstrated the potential of carbon dots for bioimaging applications, highlighting their unique fluorescent properties, high resistance to photobleaching, low cytotoxicity, and enhanced aqueous solubility. In their research, carbon dots were synthesized using carbon soot and nitric acid. The resulting blue and yellow fluorescent carbon dots were then applied to HepG2 cells, where they successfully facilitated bioimaging (Ray et al., 2009). In the study by Ray et al. (2009), HepG2 cells are commonly utilized in bioimaging experiments due to their compatibility with in vitro studies. Carbon dots were applied to these cells to observe cellular interactions, uptake mechanisms, and track specific cellular processes using fluorescence microscopy. The carbon dots emit strong fluorescence when exposed to UV light, making it easy to track cells and molecules, and thus, are highly suitable for visualization under a microscope. This research focuses on synthesizing carbon dots from corn husks (CH-CDs) using a microwave-assisted method, exploring the effects of varying microwave power levels of 450 W, 600 W, 750 W, and 900 W. Corn husks, a byproduct of corn processing, represent an abundant and sustainable carbon source, making this approach not only environmentally friendly but also economically viable. Composed primarily of hemicellulose, cellulose, and lignin, biomass has been widely used as precursors to produce high-value carbon-based products, from bulk structures to nanoscale, including carbon materials, chemicals, and biofuels

(Aswathi et al., 2022). The shift in material research towards utilizing renewable resources and implementing waste-reduction approaches has emerged as a promising route to maintaining sustainability (Adeola et al., 2023). In alignment with the 'Twelve Principles of Green Chemistry', researchers and industries are highly encouraged to develop synthetic methods that reduce environmental impact and eliminate the use of hazardous reagents (Zhu et al., 2019). Hence, this work aims to address an existing gap in understanding how these different power levels influence the properties of the synthesized carbon dots, particularly in terms of their stability, surface functionalization, and fluorescence characteristics.

II. EXPERIMENTAL PROCEDURE

The experimental procedure is outlined schematically in Figure 1, which illustrates the key stages of the synthesis and characterization of corn husk derived carbon dots (CH-CDs). The process involved the preparation of the precursor material, synthesis of carbon dots under varied microwave power conditions, and subsequent characterization of the synthesized CH-CDs to analyze their structural, optical, and surface properties. The detailed methodology is described in the following subsections.

A. Materials

Acetone (C_3H_6O,99.5%) and ethanol (C_2H_6O,99.8%) were purchased from Sigma-Aldrich Co. LLC. Corn husks were procured locally from household waste in the Shah Alam and Kuala Lumpur regions of Malaysia and were washed thoroughly prior air-dried. Distilled water was the synthesis solvent.

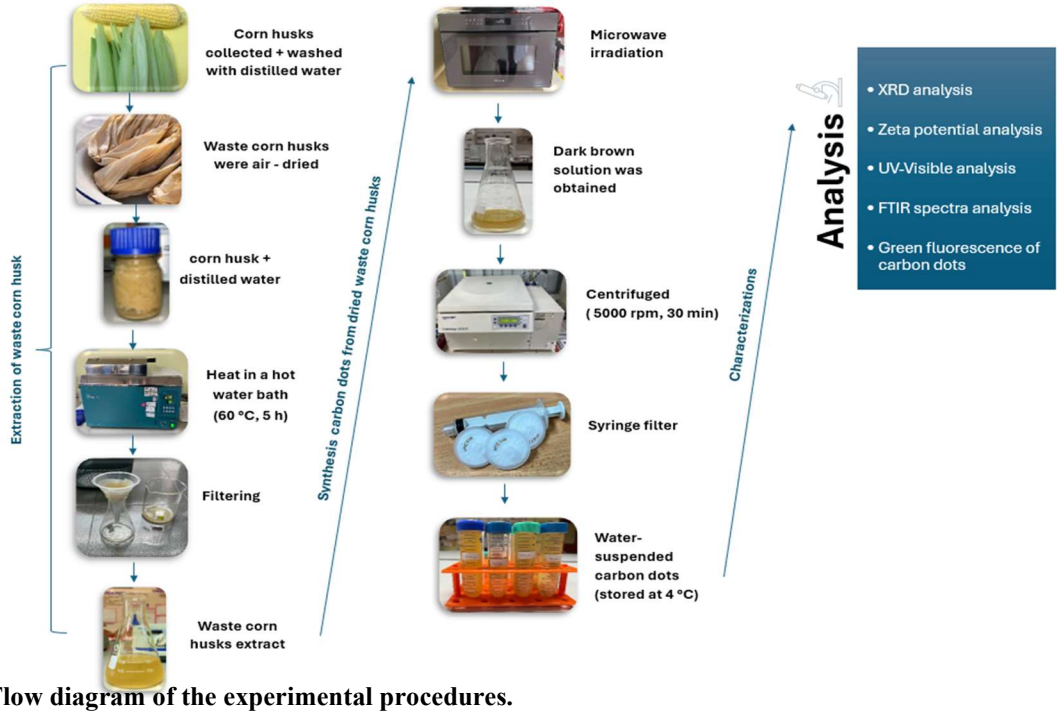


Figure 1: Flow diagram of the experimental procedures.

B. Extraction of Waste corn husk

The corn husk-carbon dots (CH-CDs) were prepared by extracting waste corn husk as the carbon precursor, through a greener synthetic route with different power levels of microwave-assisted method. Initially, the dried waste corn husks were milled using a cutting miller into coarse powder and stored. 20 g of corn husk was weighed and added to 200 mL of distilled water. The aqueous extract of corn husks was obtained by decoction, heating the solution in a hot water bath at 60 °C for 5 hours. The resulting mixture was allowed to cool down and filtered through muslin cloth and Grade I Whatman filter paper. The obtained waste corn husks extract was stored at 4 °C (Thokchom et al., 2023).

C. Synthesis of carbon dots from dried waste corn husk

The CH-CDs were synthesized by utilizing 150 mL of waste corn husk aqueous extract irradiated at 450 W, 600 W, 750 W, and 900 W for 10 minutes in a domestic microwave (SAMSUNG MC35R8088LV/SM) using a 250 mL conical flask. After cooling to room temperature, the mixtures were centrifuged (Centrifuge 5810 R) at 5000 rpm for 30 minutes, separating larger particles and filtration using a 0.22 µm syringe filter to collect the carbon dots containing supernatant. Water-suspended carbon dots were stored at 4 °C. A slight modification of the procedures referred to the study conducted by Thokchom et al. (2023) on the irradiation power level was made accordingly.

D. Characterization Technique

A comprehensive characterization technique was employed to analyse the structural, chemical, optical, and electrochemical properties of the corn husk samples and carbon dots. The structural properties were examined using X-ray diffraction (XRD) with a Rigaku Miniflex diffractometer at room temperature, with measurements conducted over a 2θ range of 5˚ to 40˚, employing Cu Kα radiation (λ = 0.154 nm)

at 40 kV and 30 mA. The zeta potential was determined using a Zeta Potential Analyzer (Nano-ZS90, Malvern) to quantify the electrostatic repulsion between similarly charged particles within the dispersion. Ultraviolet-visible (UV-Vis) spectroscopy performed using an Agilent Technologies CARY60 UV-Vis spectrometer, measured the wavelength and intensity of light absorbed by the sample, covering a range of 200–600 nm. The fluorescence properties of the carbon dots in the solution were assessed under UV irradiation. Finally, Fourier Transform Infrared (FTIR) spectroscopy (PerkinElmer, Spectrum One FTIR Spectrometer) identified the functional groups in the carbon dots, with wavenumbers ranging from 4000 cm^{-1} to 1000 cm^{-1}.

III. RESULTS AND DISCUSSIONS

A. Waste corn husk extracts

The extract obtained through the developed extraction process was effectively preserved at 4°C, successfully preventing microbial activity and chemical degradation. This critical step ensured the extract's stability and maintained its bioactive properties for further synthesis processes. The low-temperature storage significantly minimized enzymatic and oxidative reactions, which are known to degrade key bioactive compounds, thereby preserving the integrity of the extract. Additionally, the settling of particulate matter during storage resulted in a clearer supernatant, a vital improvement that enhanced the efficiency of filtration and ultimately improved the purity of the extract. These observations emphasize the importance of proper extract handling to ensure optimal performance in subsequent applications.

B. Macroscopic properties of carbon dots

The microwave-assisted synthesis of carbon dots (CH-CDs) extracts was achieved through a microwave irradiation mechanism that utilized dielectric heating. In this process, the electromagnetic field interacted with the carbon-rich components of the extract, actively facilitating the carbonization process. The corn husk extract, as confirmed by prior studies, is naturally enriched with bioactive compounds such as triterpenes (madecassoside, asiaticoside, madasiatic acid, asiatic acid), phenolic compounds, polyacetylenes, carbohydrates, and amino acids (Thokchom et al., 2023). These compounds played a dual role, serving not only as the carbon source but also as inherent passivation and functionalization agents, eliminating the need for external chemical reagents. The formation of CH-CDs was clearly evidenced by a notable color transition in the extract, shifting from pale to dark brown during the microwave treatment, as shown in Figure 2. This color change signifies the carbonization of organic components in the extract. This observation is consistent with prior work by Amber Jennings et al. (2021), which reported similar visual cues during carbon dot formation. Additionally, the fluorescence behavior of the synthesized CH-CDs under UV light confirmed their successful formation, exhibiting characteristic emissions indicative of carbon dot structures. These results provide strong evidence of the efficacy of the microwave-assisted synthesis process in converting waste biomass into functional nanomaterials.

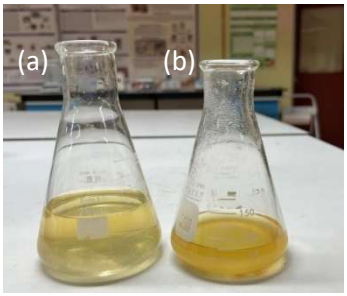


Figure 2: Colour changes of carbon dots observed (a) Before (b) After microwave-irradiation.

C. Amorphous characteristics of corn husk

The primary characteristic of the diffractogram in Figure 3 clearly indicates that the sample predominantly consists of amorphous material, as demonstrated by the broad peaks around $2\theta = 21.46^{\circ}$. This pattern mirrors earlier findings on a corn husk, which observed a similar diffraction pattern at $2\theta = 22.6^{\circ}$, corresponding to the (002) crystallographic plane, representing both the semi-crystalline and amorphous regions (Mendes et al., 2015; Setiawan et al., 2024). Natural fibers, primarily composed of cellulose, hemicellulose, and lignin, are known to exhibit both crystalline and amorphous properties (Syamani et al., 2015). In biomass, cellulose mainly constitutes the crystalline regions, while hemicellulose and lignin form the amorphous segments. Additionally, defects within cellulose crystallites further contribute to the amorphous content present in lignocellulosic biomass.

The amorphous phase of corn husk contributes to the formation of amorphous carbon dots, as Tong et al. (2014) demonstrated. In their study, amorphous carbon dots were synthesized using a hydrothermal process with citric acid and hyperbranched poly (amino amine) (HPAA). The XRD analysis showed a broad peak at $2\theta = 19.15°$, corresponding to an interplanar spacing of around 0.46 nm, indicating the presence of amorphous carbon (Tong et al., 2014). These carbon dots exhibited excellent fluorescence properties, including excitation-dependent fluorescence, with a quantum yield (QY) of 17.1% in an aqueous solution. Similarly, Bhaisare et al. (2015) reported that the X-ray diffraction pattern of carbon dots synthesized from citric acid through microwave carbonization displayed a broad peak centered around 20° (2θ), further confirming their primarily amorphous nature.

This disordered structure contributes to the fluorescence and optical properties of the carbon dots, making them highly suitable for applications in bioimaging and sensing technologies. The similarity in the diffraction patterns with other studies also benchmarks the reliability of the current synthesis method in producing high-quality amorphous carbon dots from corn husk biomass.

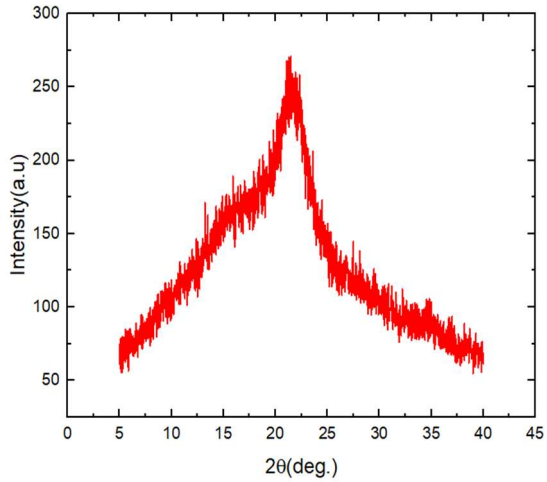


Figure 3: Spectra of XRD analysis of corn husk.

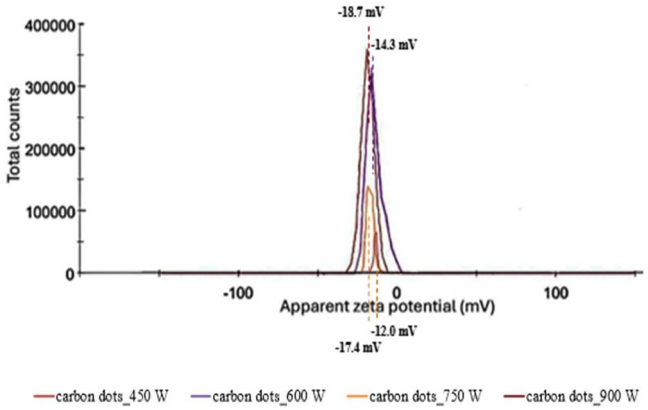


Figure 4: Graphs of zeta potential analysis of carbon dots irradiated at 450 W, 600 W, 750 W and 900 W.

D. Surface charge of carbon dots

The correlation between power levels and zeta potential values is presented in Figure 4. The results obtained from the zeta potential analysis of corn husk-carbon dots (CH-CDs) synthesized at different power levels (450 W, 600 W, 750 W, 900 W) reveal a significant impact of microwave power on the surface charge and stability of the nanoparticles. The zeta potential values exhibited a change trend with increasing power levels, indicating a shift in the surface properties of the CH-CDs. Specifically, higher irradiation power levels resulted in more negative zeta potential values, suggesting enhanced stability in the dispersed system due to increased repulsive forces between particles (Naik et al., 2020). This observation implies that the microwave power level plays a crucial role in determining the surface characteristics of the CH-CDs, which can have implications for their performance in various applications. The observed decrease in zeta potential with increasing power levels indicates stronger electrostatic repulsion between particles, contributing to improved dispersion and stability of the carbon dots (Sivasankaran et al., 2017). As depicted in Figure 4, CH-CDs synthesized at 450 W exhibit a zeta potential of -12.0 mV, which closely aligns with the value reported by Gedda et al. (2023) of -11.0 mV. Referring to the studies done by Kundu et al. (2023), the aqueous dispersion of carbon dots irradiated at 300 W in 5 minutes, exhibited a zeta potential value of -17.5 mV, indicating the presence of a high density of negatively charged carboxylic groups on the surface of the carbon quantum dots. This negative zeta potential value confirms the strong electrostatic repulsion between the particles, contributing to the excellent stability of the solution (Zhu et al., 2019).

E. Uv-vis analysis of carbon dots

The UV-Vis spectroscopy analysis of carbon dots synthesized at varying power levels provides crucial information about their optical properties. The absorption spectrum obtained from UV-Vis analysis reveals the absorption behaviour of the carbon dots in the UV and visible light regions. Referring to Figure 5, a sharp absorption edge at 292 nm indicates the presence of electronic transitions, specifically the n-π* transition corresponding to the C=O bond in the carbon core of the carbon dots (Huang et al., 2018). Additionally, the weaker absorption peak between 300 nm and 360 nm is attributed to the transition from π-π* of the C=C conjugated bond on the carbon dot surface. The continuous and broad absorption observed in the visible light region signifies the absorption of carbon dots particles at various wavelengths, reflecting their optical characteristics (Yadav et al., 2023).

The differences in absorbance intensity at various wavelengths highlight the impact of irradiation power in influencing the synthesis and properties of carbon dots. For instance, carbon dots irradiated at 450 W exhibit the lowest absorbance, measured at 1.453 abs, as shown in Figure 5. This finding suggests a relatively lower concentration or less effective formation of carbon dots at this power level. As the power increases to 600 W and 750 W, the absorbance also increases by 0.165 abs, indicating enhanced carbonization. This improvement likely results in a higher concentration of carbon dots or better passivation of surface defects, which in turn enhances light absorption (Aji et al., 2017). The trend continues with carbon dots irradiated at 900 W, which show the highest absorbance among all the samples.

A similar trend was observed in the study by Farsi et al. (2022), where increasing microwave power broadened the absorbance spectra, indicating enhanced optical properties (Zakaria et al., 2022). These improvements are attributed to a higher density of carbon dots and notable changes in their surface chemistry. The increased energy input at higher power levels likely facilitates more effective surface functionalization or passivation, reducing non-radiative recombination processes and further enhancing the optical behaviour of the carbon dots (Xia et al., 2019; Titirici et al., 2012).

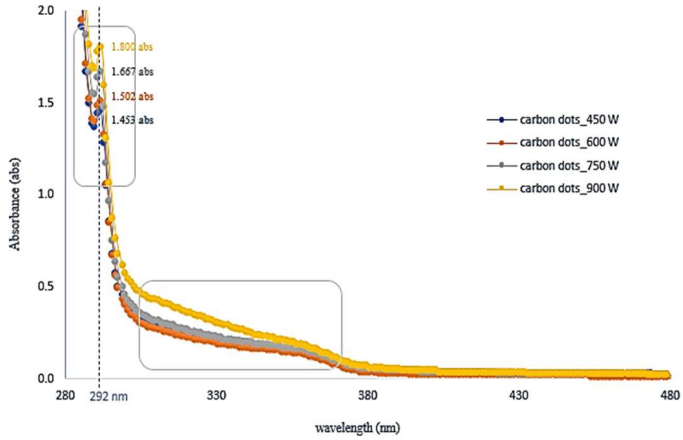


Figure 5: UV-VIS analysis of carbon dots irradiated at 450 W, 600 W, 750 W and 900 W.

F. Green fluorescence of carbon dots

The irradiation power during the synthesis of carbon dots (CDs) is crucial in determining their fluorescence properties, particularly green emission. Most carbon dots exhibit blue and green fluorescence, showing excitation-dependent behavior due to their varied size and composition. Figure 6 (a) illustrates that pale brownish carbon dots synthesized under different power levels look identical under visible light, with one representative sample shown. Exposed under UV light, green fluorescence was observed, confirming that corn husk biomass was successfully converted into carbon dots as in Figure 6 (b). Among the samples, carbon dots synthesized at the highest power level (900 W) exhibit the brightest green fluorescence, while those produced at a lower power level (450 W) display weaker green fluorescence, attributed to incomplete carbonization.

At lower power levels, such as 450 W, the energy provided is insufficient for thorough carbonization. This results in the formation of smaller carbon dots with fewer surface defects or functional groups, leading to weaker green fluorescence. The incomplete surface passivation and suboptimal structural properties of these carbon dots further contribute to their reduced fluorescence intensity (Ren et al., 2025). As the power increases to 600 W and 750 W, the reaction proceeds more efficiently, producing carbon dots with more uniform sizes and better carbonization. The surface defects and functional groups, such as carboxyl or hydroxyl groups become more abundant, enhancing the quantum yield and fluorescence stability (Diwan et al., 2024). At the highest power level of 900 W, the synthesis process achieves optimal efficiency, yielding carbon dots with sizes and surface characteristics that promote a high quantum yield. The resulting fluorescence intensity peaks at this level, producing carbon dots that emit a bright and consistent green glow under UV light, as observed in Figure 6(b).

As the irradiation power increases, so does the intensity of green fluorescence. This trend aligns with previous research by Al Farsi et al. (2022), which demonstrated that higher microwave power increases the density of surface functional groups, positively affecting photoluminescence. The elevated thermal energy enhances the graphitization of carbon dots, leading to more defined energy levels and higher fluorescence intensity. Moreover, incomplete carbonization at lower power levels results in larger carbon dots with a smaller bandgap, causing red-shifted emission due to less energetic electronic transitions (Sutanto et al., 2020). Insufficient power also restricts surface functionalization, increasing non-radiative recombination pathways and further reducing photoluminescence intensity (Hu et al., 2021).

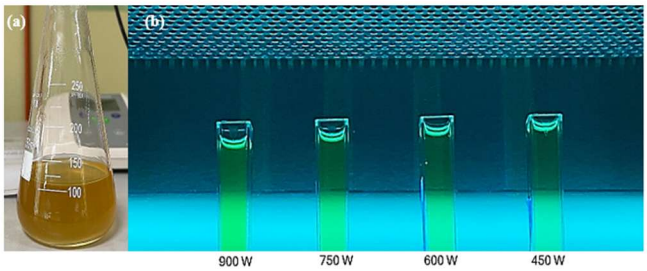


Figure 6: Carbon dots observed under (a) visible light (b) UV light.

G. Functional groups of carbon dots

Fourier-transform infrared (FTIR) spectroscopy analysis offers detailed insights into the functional groups present on the surface of carbon dots synthesized using microwave irradiation. The FTIR spectra display characteristic absorption bands corresponding to different chemical bonds, providing information about the surface chemistry of the carbon dots. Figure 7 illustrates the characteristic absorption bands. The FTIR spectrum for CH-CDs irradiated at 450 W shows distinct peaks at 3253.88 cm^{-1}, indicating O-H stretching vibrations, suggesting the presence of hydroxyl groups. The peak at 2359.92 cm^{-1} corresponds to C≡N stretching vibrations, while the peak at 2228.95 cm^{-1} attributed to aromatic and conjugated molecules of nitrile groups. Another peak at 2074.31 cm^{-1} may indicate the presence of C≡C stretching. A prominent peak at 1635.08 cm^{-1} suggests the presence of C=O stretching vibrations, indicating carbonyl groups.

The spectrum of CH-CDs irradiated at 600 W shows a similar broad O-H stretching vibration at 3252.35 cm^{-1} which indicate the hydrophilic functional group. The peak at 2448.71 cm^{-1} suggests C≡N stretching, while peaks at 2118.29 cm^{-1} and 1833 cm^{-1} indicate the presence of nitrile and other carbon-containing groups. The peak at 1635.05 cm^{-1}, similar to 450 W, indicates C=O stretching vibrations. The peaks at 1350 cm^{-1} and 1082 cm^{-1} can be attributed to C-H bending and C-O stretching vibrations, respectively, suggesting the presence of aliphatic groups and alcohol or ester functionalities. The appearance of peaks at 1350 cm^{-1} and 1082 cm^{-1} in the 600 W spectrum suggests aliphatic and alcohol or ester functionalities, which may result from partial oxidation or other surface modifications at this power level.

At 750 W, the FTIR spectrum shows a slight shift in the O-H stretching vibration to 3270.04 cm^{-1}, indicating changes in the hydroxyl groups. The peaks at 2756 cm^{-1} and 2246.74 cm^{-1} correspond to C-H and C≡N stretching vibrations, respectively. The peak at 1901 cm^{-1} suggests the presence of carbonyl groups. The significant peak at 1635.99 cm^{-1} indicates C=O stretching vibrations, while the peaks at 1072

cm^{-1} suggest C-O stretching vibrations, similar to the lower power irradiations.

The spectrum for CH-CDs irradiated at 900 W exhibits an O-H stretching vibration at 3250.13 cm^{-1}. The peaks at 2545 cm^{-1} and 2357.98 cm^{-1} suggest the presence of C≡N stretching vibrations. The peaks at 1981.24 cm^{-1} indicate the presence of alkyne. The peak at 1635.76 cm^{-1}, consistent across all spectra, indicates C=O stretching vibrations. The peak at 1046 cm^{-1} can be attributed to C-O stretching vibrations, similar to other irradiation levels.

The FTIR spectrum reveals the formation of unsaturated carbon structures and the presence of oxygen-rich functional groups on the surface of the synthesized CH-CDs. Peaks at specific wavenumbers indicate the presence of functional groups such as C=C stretching for aromatic compounds, C-O stretch, and C=O bonds similar to the findings by Aji et al. (2017). The FTIR spectra across the different irradiation powers reveal a consistent presence of O-H and C=O functional groups, indicating that the hydroxyl and carbonyl groups are stable under varying irradiation powers.

According to Sutanto et al. (2020), the higher the amount of hydroxyl groups, the higher the stability of carbon dots in aqueous solution. FTIR spectra analysis shows distinct O-H stretching vibrations at approximately 3253.88 cm^{-1} for carbon dots irradiated at 450 W, with similar peaks observed at 3252.35 cm^{-1} for those at 600 W. As the irradiation power increases to 750 W, a slight shift to 3270.04 cm^{-1} is noted, indicating potential changes in the hydroxyl groups. At the highest power of 900 W, the O-H stretching vibration is recorded at 3250.13 cm^{-1}, suggesting that hydroxyl groups remain stable across varying conditions. The consistent presence of these peaks, along with the slight shifts at higher power levels, implies that increased microwave irradiation enhances the amount of hydroxyl functional groups in the carbon dots. These results indicate that the irradiation power significantly influences the surface chemistry of the carbon dots, potentially affecting their solubility and overall functionality in applications such as sensing, catalysis, or drug delivery (Adaikalapandi et al., 2024).

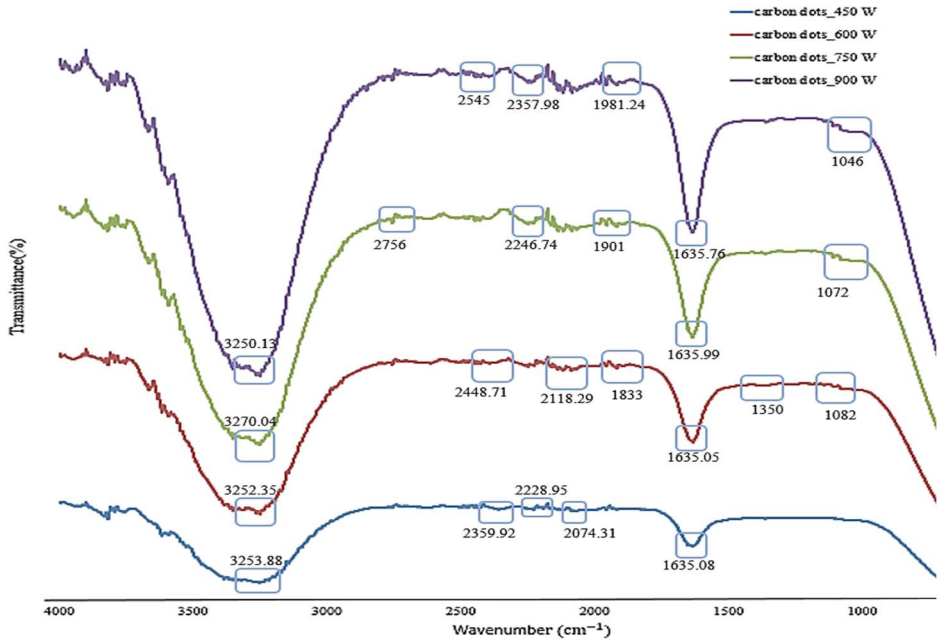


Figure 7: Graphs of FTIR spectra analysis of carbon dots irradiated at 450 W, 600 W, 750 W and 900 W.

IV. CONCLUSION

This study explored the microwave-assisted synthesis of carbon dots (CH-CDs) derived from corn husk, emphasizing the impact of varying power levels on their structural, optical, and stability properties. At higher microwave powers, particularly 900 W, the carbon dots exhibited improved optical properties, including stronger UV-Vis absorbance at 292 nm and spectral broadening, suggesting higher concentration and enhanced surface characteristics. Zeta potential analysis revealed more negative values at increased power levels, indicating greater stability due to stronger repulsive forces between particles. FTIR analysis confirmed the consistent presence of hydroxyl (O-H) and carbonyl (C=O) groups across all power levels, correlating higher hydroxyl group concentrations with better stability in aqueous solutions. Additionally, higher power levels promoted the formation of complex carbon structures, as evidenced by the increased prominence of nitrile (C≡N) and alkyne (C≡C) groups. Collectively, the findings demonstrate that controlling microwave power is critical for optimizing the synthesis process, achieving desirable surface charge, stability, and optical properties in CH-CDs. Future research incorporating Transmission Electron Microscopy (TEM) significantly enhance the characterization of CH-CDs. By integrating TEM into the analytical framework will strengthen the structural

analysis of CH-CDs and unlock the potential in various nanotechnology applications.

AUTHOR CONTRIBUTIONS

N. Zulkifli: Conceptualization, Methodology, Writing – original draft. **H. Alwi:** Supervision, Writing – original draft. **S. M. Sauid:** Supervision, Writing – review & editing. **M. F. Sarulan.:** Monitoring, Validation. **N. Wahid:** Software, Validation.

REFERENCES

Adaikalapandi, S.; T. D. Thangadurai; N. Manjubaashini; D. Nataraj; T. S. Babu and S. M. Kumar (2024). Bamboo stem biomass waste-derived excitation-dependent carbon dots for nanomolar detection of fungicide dodine in real samples and their pH-sensitive bacterial interaction studies. *Diamond and Related Materials*, *141*, 110692.

Adeola, A. O.; M. P. Duarte and R. Naccache (2023). Microwave-assisted synthesis of carbon-based nanomaterials from biobased resources for water treatment applications: emerging trends and prospects. *Frontiers in Carbon*, *2*, 1220021.

Aji, M. P.; Susanto; P. A. Wiguna and Sulhadi (2017). Facile synthesis of luminescent carbon dots from mangosteen peel by pyrolysis method. *Journal of Theoretical and Applied Physics*, *11*(2), 119–126.

Al Farsi, B.; R. G. S. Sofin; H. Al Shidhani; E. S. I. El-Shafey; A. S. Al-Hosni; F. Al Marzouqi; A. Issac; A. Al Nabhani and O. K. Abou-Zied (2022). The effect of microwave power level and post-synthesis annealing treatment on oxygen-based functional groups present on carbon quantum dots. *Journal of Luminescence*, 252, 119326.

Aswathi, V. P.; S. Meera; C. G. A. Maria and M. Nidhin (2022). Green synthesis of nanoparticles from biodegradable waste extracts and their applications: a critical review. *Nanotechnology for Environmental Engineering*, *8*(2), 377–397.

Nimibofa, A.; E. A. Newton; A. Y. Cyprain and W. Donbebe (2018). Fullerenes: Synthesis and Applications. *Journal of Materials Science Research. 7*(3), 22.

Bhakta, P. and Barthunia, B. (2020). Fullerene and its applications: A review. *Journal of Indian Academy of Oral Medicine and Radiology*. *32*(2). 159-163.

Bhaisare, M. L.; A. Talib; M. S. Khan; S. Pandey and H. F. Wu (2015). Synthesis of fluorescent carbon dots via microwave carbonization of citric acid in presence of tetraoctylammonium ion, and their application to cellular bioimaging. *Microchimica Acta*, *182*(13–14), 2173–2181.

Brichkin, S. B.; V. F. Razumov; N. Akma Mahat and S. A. Shamsudin (2020). Blue luminescence carbon quantum dots derived from oil palm empty fruit bunch biomass. *IOP Conference Series: Materials Science and Engineering*, *736*(5), 052001.

Cao, L.; Y. S. Ang; Q. Wu and L. K. Ang (2020). Electronic properties and spintronic applications of carbon phosphide nanoribbons. *Physical Review B, 101*(3), 035422.

Cui, L.; X. Ren; M. Sun; H. Liu and L. Xia (2021). Carbon Dots: Synthesis, Properties and Applications. *Nanomaterials*, *11*(12), 3419.

Diwan, I.; G. K. Tripathi and P. S. Khare, (2024). Synthesis of green fluorescent, energy efficient nitrogen doped carbon quantum dots. *Optik*, *303*, 171725.

Frese, N.; S. T. Mitchell; C. Neumann; A. Bowers; A. Gölzhäuser and K. Sattler (2016). Fundamental properties of high-quality carbon nanofoam: from low to high density. *Beilstein Journal of Nanotechnology*, *7*(1), 2065.

Forest, C.; P. Chaumont; P. Cassagnau; B. Swoboda; and P. Sonntag (2015). Polymer nano-foams for insulating applications prepared from CO2 foaming. *Progress in Polymer Science, 41*, 122–145.

Gedda, G.; S. A. Sankaranarayanan; C. L. Putta; K. K. Gudimella; A. K. Rengan; and W. M. Girma (2023). Green synthesis of multi-functional carbon dots from medicinal plant leaves for antimicrobial, antioxidant, and bioimaging applications. *Scientific Reports*, *13*(1), 1–9.

Han, S.; J. Sun; S. He; M. Tang; and R. Chai (2019). The application of graphene-based biomaterials in biomedicine. *American journal of translational research*, *11*(6), 3246–3260.

Huang, Q.; Q. Li; Y. Chen; L. Tong; X. Lin; J. Zhu and Q. Tong (2018). High quantum yield nitrogen-doped carbon dots: green synthesis and application as “off-on” fluorescent sensors for the determination of Fe3+ and adenosine triphosphate in biological samples. *Sensors and Actuators B: Chemical*, *276*, 82–88.

Hu, D.; K. H. Lin; Y. Xu; M. Kajiyama; M. Neves; K. Ogawa and T. Enomae (2021). Microwave-assisted synthesis of fluorescent carbon dots from nanocellulose for dual-metal ion-sensor probe: Fe (III) and Mn (II). *Cellulose*, *28*(15), 9705-9724.

Kang, C.; Y. Huang; H. Yang; X. F. Yan and Z. P. Chen (2020). A Review of Carbon Dots Produced from Biomass Wastes. *Nanomaterials 2020*, 10(11), 2316.

Kundu, A.; S. Basu and B. Maity (2023). Upcycling Waste: Citrus limon Peel-Derived Carbon Quantum Dots for Sensitive Detection of Tetracycline in the Nanomolar Range. *ACS omega*, *8*(39), 36449–36459.

Kurian, M. and Paul, A. (2021). Recent trends in the use of green sources for carbon dot synthesis–A short review. *Carbon Trends*, *3*, 100032.

Liu, S.; C. Ma; M. G. Ma and J. F. Li (2018). Recent Advances in Carbon Nanomaterials Derived from Biomass. *Science of Advanced Materials*, *11*(1), 5–17.

Louis, B.; D. Bégin; M.J. Ledoux and C. Pham-Huu (2009). Advances in the use of carbon nanomaterials in catalysis. *Ordered porous solids,* 621–649.

Mendes, C. C. A.; F. A. O. Adnet; M. C. A. Leite; C. Furtado and A. M. F. Sousa (2015). Chemical, Physical, Mechanical, Thermal And Morphological Characterization Of Corn Husk Residue. *Cellulose Chemistry and Technology, 49*(9), 727–735.

Mohamed, A. (2019). Synthesis, characterization, and applications of carbon nanofibers. *Carbon-based nanofillers and their rubber nanocomposites*, 243–257.

Naik, G. G.; M. B. Alam; V. Pandey; D. Mohapatra; P. K. Dubey; A. S. Parmar and A. N. Sahu (2020). Multi-Functional Carbon Dots from an Ayurvedic Medicinal Plant for Cancer Cell Bioimaging Applications. *Journal of Fluorescence, 30*(2), 407–418.

Olabi, A. G.; M. A. Abdelkareem; T. Wilberforce and E. T. Sayed (2021). Application of graphene in energy storage device – A review. *Renewable and Sustainable Energy Reviews, 135*, 110026

Peng, L. M.; Z. Zhang and S. Wang (2014). Carbon nanotube electronics: Recent advances. *Materials Today, 17*(9), 433–442.

Poklonski, N. A.; E. F. Kislyakov; S. A. Vyrko; O. N. Bubel and S. V. Ratkevich (2012). Electronic band structure and magnetic states of zigzag graphene nanoribbons: quantum chemical calculations. *Journal of Nanophotonics*, *6*(1), 061712.

P**orto, L. S.; D. N. Silva; A. E. F. Oliveira; A. C. Pereira and K. B. Borges (2020).** Carbon nanomaterials: Synthesis and applications to development of electrochemical sensors in determination of drugs and compounds of clinical interest. *Reviews in Analytical Chemistry*, *38*(3), 20190017.

Ray, S. C.; A. Saha; N. R. Jana and R. Sarkar (2009). Fluorescent carbon nanoparticles: Synthesis, characterization, and bioimaging application. *Journal of Physical Chemistry, 113*(43), 18546–18551.

Ren, C.; C. Tian; M. Zhang; F. Li; Y. Li; F. Zhang; J. Zhang; G. Chen and J. Tang (2025). The fluorescence properties of nitrogen-doped carbon dots by microwave green approaches. *Journal of Molecular Structure*, *1319*, 139364.

Saeed, M.; M. Muneer; M. K. K. Khosa; N. Akram; S. Khalid; M. Adeel; A. Nisar and S. Sherazi (2019). Azadirachta indica leaves extract assisted green synthesis of Ag-TiO2 for degradation of Methylene blue and Rhodamine B dyes in aqueous medium. *Green Processing and Synthesis*, *8*(1), 659–666.

Setiawan, A.; R. N. M. Mahfud; N. E. Mayangsari; D. R. Widiana; A. P. Iswara and D. Dermawan (2024). The potential of using sweet corn (Zea mays Saccharata) husk waste as a source for biodegradable plastics. *Industrial Crops and Products*, *208*, 117760.

Sharma, A. and Das, J. (2019). Small molecules derived carbon dots: synthesis and applications in sensing, catalysis, imaging, and biomedicine. *Journal of Nanobiotechnology, 17*(1), 1–24.

Sim, L. C.; J. Y. Tai; J. M. Khor; J. L. Wong; J. Y. Lee; K. H. Leong; P. Saravanan and A.A. Aziz (2019). Carbon Dots Synthesized from Green Precursors with an Amplified Photoluminescence: Synthesis, Characterization, and Its Application. *Plant Nanobionics: Volume 2, Nanotechnology in the Life Sciences*, *2*, 1–33.

Sivasankaran, U.; S. Jesny; A. R. Jose; and K. Girish Kumar (2017). Fluorescence determination of glutathione using tissue paper-derived carbon dots as fluorophores. *Analytical Sciences: The International Journal of the Japan Society for Analytical Chemistry, 33*(3), 281–285.

Soledad-Flores, O.; S. J. Bailón-Ruiz and F. Román-Velázquez (2024). Rapid Synthesis of Non-Toxic, Water-Stable Carbon Dots Using Microwave Irradiation. *Micro*, *4*(4), 659-669.

Soni, H. and Pamidimukkala, P. S. (2018). Green synthesis of N, S co-doped carbon quantum dots from triflic acid treated palm shell waste and their application in nitrophenol sensing. *Materials Research Bulletin, 108*, 250–254.

Sutanto, H.; I. Alkian; N. Romanda; I. W. L. Lewa; I. Marhaendrajaya and P. Triadyaksa (2020). High green-emission carbon dots and its optical properties: Microwave power effect. *AIP Advances, 10*(5), 55008.

Syamani, F. A. and Suryani, A. (2015). Changes in Oil Palm Frond Fiber Morphology; Cellulose Crystallinity and Chemical Functional Groups during Cellulose Extraction Phases. *Chemistry and Materials Research, 7*(3), 105–114.

Thiruketheeswaranathan, S. and Somasiri, W. (2021). Comparative Study of Neem (Azadirachta Indica) Leaf, Bark and Seed as An Adsorbent for Dye, Methylene Blue Removal. *International Journal of Applied Research 2019*, *5*(4), 434-441

Thokchom, B.; S. M. Bhavi; M. B. Abbigeri; A. K. Shettar and R. B. Yarajarla (2023). Green synthesis, characterization and biomedical applications of Centella asiatica-derived carbon dots. *Carbon Letters*, *33*(4), 1057–1071.

Titirici, M. M.; R. J. White; C. Falco and M. Sevilla (2012). Black perspectives for a green future: Hydrothermal carbons for environment protection and energy storage. *Energy and Environmental Science, 5*(5), 6796–6822.

Tong, G.; J. Wang; R. Wang; X. Guo; L. He; F. Qiu; G. Wang; B. Zhu; X. Zhu and T. Liu (2014). Amorphous carbon dots with high two-photon fluorescence for cellular imaging passivated by hyperbranched poly(amino amine). *Journal of Materials Chemistry B*, *3*(4), 700–706.

Xia, C.; S. Zhu; T. Feng; M. Yang; B. Yang; C. Xia; T. Feng; M. Yang; B. Yang and S. Zhu (2019). Evolution and Synthesis of Carbon Dots: From Carbon Dots to Carbonized Polymer Dots. *Advanced Science*, *6*(23), 1901316.

Yadav, P. K.; S. Chandra; V. Kumar; D. Kumar and S. H. Hasan (2023). Carbon Quantum Dots: Synthesis, Structure, Properties, and Catalytic Applications for Organic Synthesis. *Catalysts*, *13*(2), 422.

Yang, X.; Y. Chen; C. Zhang; G. Duan and S. Jiang (2023). Electrospun carbon nanofibers and their reinforced composites: Preparation, modification, applications, and perspectives. *Composites Part B: Engineering,* 249, 110386.

Zakaria, N. Z. J.; S. Rozali; N. M. Mubarak and S. Ibrahim (2022). A review of the recent trend in the synthesis of carbon nanomaterials derived from oil palm by-product materials. *Biomass Conversion and Biorefinery 2022*, *14*(1), 13–44.

Zhu, X.; K. Pathakoti and H. M. Hwang (2019). Green synthesis of titanium dioxide and zinc oxide nanoparticles and their usage for antimicrobial applications and environmental remediation. *Green Synthesis, Characterization and Applications of Nanoparticles*, 223–263.